

## Effect of Modified Kaolin Clays on the Mechanical Properties of Polypropylene/Polystyrene Blends

Asha K. Krishnan, Tresa Sunitha George, R. Anjana, Newly Joseph, K. E. George

Department of Polymer Science and Rubber Technology, Cochin University of Science and Technology, Kochi, Kerala 682022, Tamil Nadu, India

Correspondence to: K. E. George (E-mail: kegeorge@cusat.ac.in)

**ABSTRACT:** Nanoclay composites based on polypropylene (PP)/polystyrene (PS) blends were prepared by melt mixing in a Thermo Haake Rheochord mixer. The effect of modified clays on the properties of nanocomposites has been studied. The degree of dispersion and morphology of nanocomposites were evaluated from X-ray diffraction and Scanning electron microscopy. Nanocomposites prepared from modified clays show improved tensile modulus and strength as compared to those prepared from unmodified clay. Vinyl silane modified nanocomposites show maximum improvement in mechanical properties, suggesting that vinyl silane provides better interfacial interaction. Thermogravimetric analysis shows improved thermal stability of PP/PS/clay nanocomposites. The dynamic mechanical analysis reveals higher storage moduli over a temperature range of 40–125°C for nanocomposites, and the extent of increase in the storage modulus is dependent on the type of clay. © 2012 Wiley Periodicals, Inc. *J. Appl. Polym. Sci.* 000: 000–000, 2012

**KEYWORDS:** mechanical properties; thermogravimetric analysis; thermoplastics; polystyrene; morphology

Received 14 February 2012; accepted 11 May 2012; published online

DOI: 10.1002/app.38043

### INTRODUCTION

Polymer-clay nanocomposites are a class of hybrid materials composed of organic polymer matrix in which layered inorganic particles with nanoscale dimension is distributed. As a result of the nanometer-scale dispersion, nanocomposites exhibit markedly improved mechanical, thermal, and physicochemical properties, decreased gas and water vapor permeability, resistance to flammability, and thermal degradation as compared with the conventional composites.<sup>1–5</sup> These nanocomposites synergistically integrate the advantages of organic polymers and those of the inorganic filler.

Polypropylene (PP) and Polystyrene (PS) are two of the most widely used commercial polymers and hence the hybridization of PP/PS blends with nanostructured fillers may be useful in generating a variety of useful materials.<sup>3</sup> PP and PS used in this study are immiscible, which leads to the formation of multiphase system with different morphology that depends on the composition of the blend, viscosity ratio of the components, interfacial tension between the two phases, and processing condition of the blends. As PP and PS are immiscible, a considerable amount of work on compatibilizing PP and PS has been done by using compatibilizers such as SBS, SEBS, SEP, and PP-*g*-PS.<sup>6–9</sup>

In recent years, the possible application of relatively cheap organoclays as compatibilizers is getting serious attention.

Organoclays are being widely used as an attractive alternative to conventional fillers. Much of the work in this area has focused on montmorillonite.<sup>10,11</sup> Hence, in this study kaolin clay with a 1 : 1 type layered structure with chemical composition  $\text{Al}_2\text{Si}_2\text{O}_5(\text{OH})_4$  is proposed to be used. It is a layered silicate mineral with one tetrahedral sheet linked through oxygen atoms to one octahedral sheet of alumina octahedral. The layers are held together via hydrogen bonds, dipolar interactions, and van der Waals forces, which result in a low intrinsic inner surface reactivity. Because of the hydrophilic character of kaolinite and hydrophobic properties of polymer the modification of kaolinite is necessary.<sup>12–14</sup> Modification was done by coupling of organosilane compounds, with two kinds of reactive groups (inorganic and organic) in a single molecule. A chemical reaction between the functional groups (such as OH) of filler and the alkoxy groups of silane is expected to occur, creating a silane-functionalized surface.<sup>15</sup> The silane grafting of clay has received much attention in recent years, both in the industry and academy. Kaolin clay so modified has many applications; it is used in paper, paint, rubber, plastics, and ceramics industries.

A comparative study of Nanocaliber 100 (unmodified kaolin clay) with two types of commercially available modified clays Nanocaliber 100 V (vinyl silane modified kaolin clay) and Nanocaliber100 A (amino silane modified kaolin clay) is proposed to be carried out.

## EXPERIMENTAL

## Materials

PP homopolymer: H 200 MA, homopolymer, with a Melt Flow index of 25 g/10 min (230°C/2.16 kg) was purchased from Reliance Industries limited, India

The PS (MFI (200°C/5 kg) is 12 g/10 min) was obtained from Supreme Petrochem, India.

Kaolin clay: Unmodified and modified kaolin clays were obtained from English India Clays Limited Veli, Thiruvananthapuram, Kerala, India. The samples had a bulk density of 0.2–0.3 g/cc and a BET (Brunauer, Emmett and Teller) specific surface area of 28–30 m<sup>2</sup>/g. The samples used were unmodified clay (Nanocaliber 100), vinyl silane modified clay (Nanocaliber 100V–N100V) and amino silane modified clay (Nanocaliber 100 A–N100A).

## Nanocomposite Preparation

PP/PS (80/20) and the nanoclays Nanocaliber 100 V, Nanocaliber 100, and Nanocaliber 100 A in varying amounts (0.44–3.5 vol %) were prepared by melt mixing using an internal mixer (Haake Rheomix 600) at 180°C with a rotor speed of 50 rpm/min, and mixing time is 8 min for each sample. After mixing the melt was pressed in a hydraulic press, cut into pieces and injection molded in a semi automatic Texiar injection molding machine (Model JIM 1 H series, 4508), for preparing test specimens for tensile and flexural testing as per relevant ASTM standards.

## Characterization

Dynamic mechanical analysis (DMA Q-800, TA instruments) was used to study the effect of nanoclays on the viscoelastic properties of PP/PS clay nanocomposites. Rectangular shaped specimens of dimension 35 × 4 × 3 mm<sup>3</sup> were used. DMA tests were conducted at a frequency of 1 Hz. A temperature ramp was run from 38 to 125°C at 3°C/min.

Thermal stability of the polymer blend/clay nanocomposites was analyzed using TGA Q-50 of TA instruments under N<sub>2</sub> atmosphere. The samples weight of about 5–7 mg was heated at a rate of 20°C/min from ambient temperature to 600°C.

The samples were analyzed in a Bruker AXS D8 Advance X-Ray Powder Diffractometer (Cu K $\alpha$  radiation) in order to find the change in basal spacing of nanocomposites. The samples were scanned in the range of 3°–80° at increment step of scanning 0.020° at a wave length of 1.5406 Å.

Tensile properties of PP/PS (80/20) blend, unmodified and modified clay nanocomposites were evaluated using Shimadzu Autograph AG-I series universal testing machine at a crosshead speed of 50 mm/min and according to ASTM D 638. The injection molded dumbbell shape specimens had an overall length of 115 mm, a width in the gauge section of 6 mm and a thickness of 3.2 ± 0.4 mm. A minimum of five samples were tested in each nanocomposite and the average results were recorded.

Flexural strength of PP/PS (80/20) blend, unmodified, and modified clay nanocomposites were measured by three point loading system using UTM (Shimadzu AG-1) with a load cell capacity according to ASTM D 790. The testing was done at a

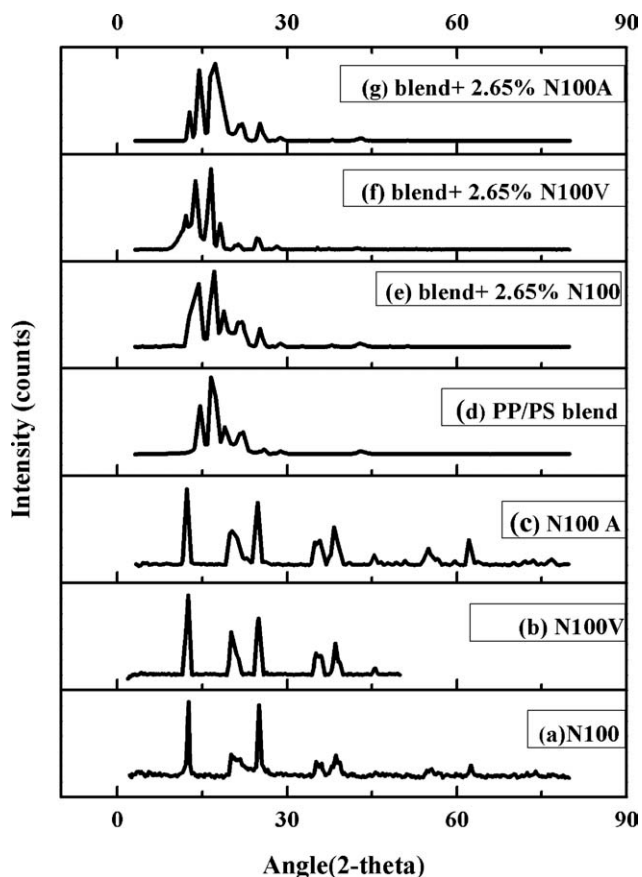


**Figure 1.** XRD patterns of (a) Nanocaliber100, (b) Nanocaliber100V, (c) Nanocaliber100A, (d) PP/PS blend, (e) PP/PS/N100, (f) PP/PS/N100V, and (g) PP/PS/N100A.

crosshead speed of 5 mm/min. Rectangular bars of dimensions 60 × 12.7 × 3.2 mm<sup>3</sup> (width × length × thickness). A minimum of five samples were tested in each nanocomposite and the average results were recorded.

Morphology of the tensile fractured surfaces of the nanocomposite specimens were investigated by using JEOL Model JSM 6390LV scanning electron microscope (SEM). The samples were subjected to gold sputtering prior to electron microscopy to give the necessary conductivity.

## RESULTS AND DISCUSSION

## X-ray Diffraction

X-ray diffraction (XRD) is extremely useful to study the structure and morphology of polymer nanocomposites. It provides information on the changes of the inter-layer spacing of the clay upon the formation of nanocomposites. The formation of an intercalated structure should result in a decrease in 2 $\theta$ , indicating an increase in the *d*-spacing. The interlayer *d*-spacing observed by XRD for polymer-clay nanocomposites has been used to describe the nanoscale dispersion of clay in the polymer matrix.<sup>16</sup> Figure 1 shows the XRD patterns of Nanocaliber 100, Nanocaliber 100 V, and Nanocaliber 100 A, PP/PS pure blend and its nanocomposites reinforced with the three types of modified clays at 2.65 vol %. Diffraction peaks that appear at 2 $\theta$  =

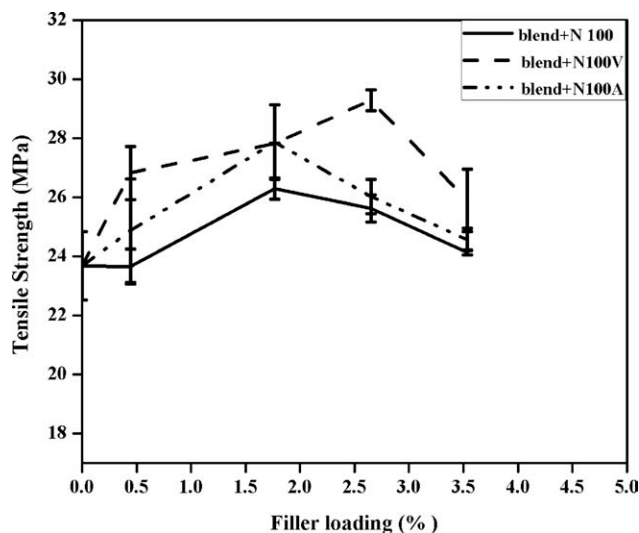


**Figure 2.** Variation of Tensile strength with different nanoclay composition in PP/PS (80/20) blend.

15°–20° corresponds to the monoclinic  $\alpha$  form of the PP. The PP/PS nanocomposites have a slightly different intensity of reflections than pure PP/PS and this indicates modification of the crystalline nature of PP in the PP/PS nanocomposite.<sup>17–19</sup> The original basal reflection peak for N 100 is 12.540°, which correspond to an intergallery spacing of 7.05329 nm and the peaks for N 100V and N 100A are at 12.442° and at 12.276°, respectively, which corresponds to an intergallery spacing of 7.10842 and 7.20406 nm. For the PP/PS/N100V nanocomposite, the characteristics peak of N100V is shifted to  $2\theta = 12.076^\circ$ , corresponding to a  $d$ -spacing of 7.3229 nm, which indicates that some PP/PS molecular chains are intercalated between the clay galleries, forming an intercalated structure. Characteristic peak for PP/PS/N100A nanocomposite is at 12.737° and has a  $d$ -spacing of 6.99454 nm and peak for PP/PS/N100 is at 12.665° having a  $d$ -spacing of 6.98918 nm. The XRD does not show any

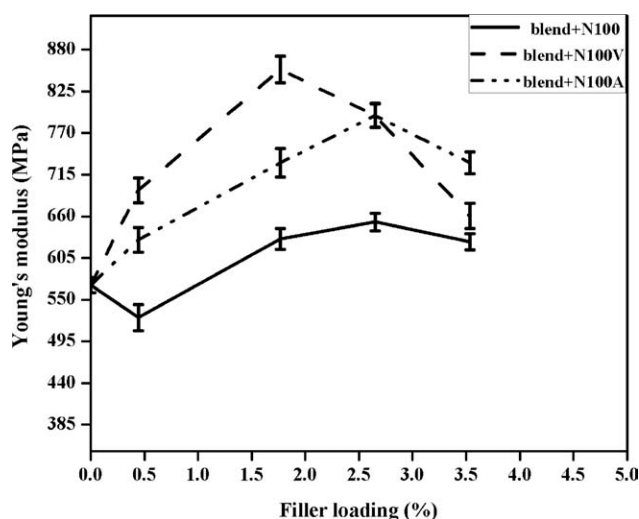


**Figure 3.** Variation of Young's modulus with different nanoclay composition in PP/PS (80/20) blend.

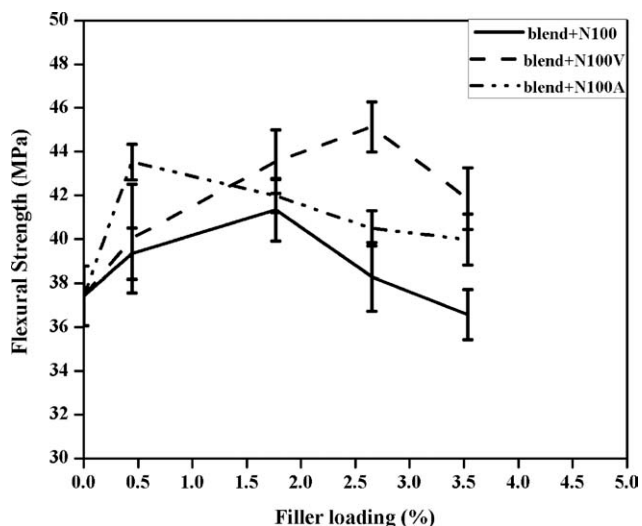


**Figure 4.** Variation of Flexural strength with different nanoclay composition in PP/PS (80/20) blend.

shift in the diffraction peak for the PP/PS/N100A and PP/PS/N100 nanocomposites. This shows that these blends can be considered as conventional microcomposites.

The extent of nanoclay intercalation in a polymer nanocomposite depends on three important factors: clay–clay interaction, polymer–surfactant interaction, and polymer–clay interaction. While surfactants can weaken clay–clay interaction so as to allow polymer interaction between clay layers, these same surfactants can also sterically hinder the access of polymer chains to the clay surface. Hence, the selection of appropriate surfactant for the polymer of interest is of utmost important in melt processing.<sup>20</sup> By incorporating surfactant with hydrophobic tails on the clay surface will efficiently reduce clay–clay interaction. During the melt blending, the presence of vinyl silane groups enhances the ability of the PP/PS chains to intercalate in between the clay galleries. This is due to the increased clay gallery distance and favorable interactions between the surfactant and the polymer molecule. Vinyl silane modified nanoclay (N 100V) is found to be more suitable for PP/PS blend.<sup>21</sup>

### Mechanical Analysis

The tensile strength and Young's modulus as a function of increasing filler loading of unmodified and the two modified nanocomposites are shown in Figures 2 and 3, respectively. Tensile properties increase initially with increasing filler loading reach a maximum and there after begin to decrease.

The insertion of the polymer chains inside the silicate layers leads to an increase in the surface area of interaction between the clay and polymer matrix thereby resulting in an increase in strength and modulus. The mechanical properties of the compatibilized polymer blends are likely to be improved compared to corresponding incompatibilized ones because of the lower interfacial tension and enhanced interfacial adhesion, which results in more efficient stress transfer between the phases during fracture.<sup>8</sup> The decrease in tensile properties, may be due to the agglomeration of clay particles. When the clay agglomerates are

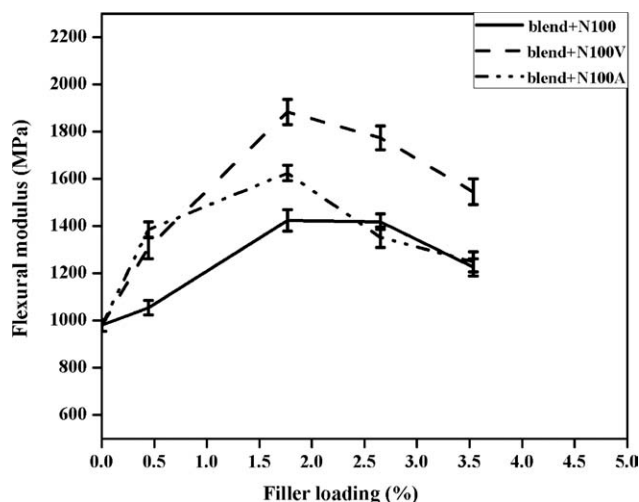


**Figure 5.** Variation of Flexural modulus with different nanoclay composition in PP/PS (80/20) blend.

present, the stress acting on a small part of the material surface would be much greater than the average stress applied to the test specimen.

Effect of organoclay type on flexural properties of nanocomposites is illustrated in Figures 4 and 5, respectively. The change of flexural strength of the samples with respect to organoclay content shows resemblance to tensile strength change. The increase in flexural strength and modulus indicates that the nanocomposites have become more rigid and less flexible. The enhancement in the mechanical properties is more pronounced with N100V. This further shows that vinyl silane modified kaolin clay (N100V) has better interaction with the polymers.

### Thermal Stability

In most cases the incorporation of clay into the polymer matrix is found to enhance the thermal stability. The thermal stability of the nanocomposites has been investigated using TGA; Table I presents the results of TGA of PP/PS nanocomposites. The temperature at which 10% degradation occurs, a measure of the onset of degradation, the temperature at which 50% degradation occurs, the midpoint of the degradation process, and the fraction of material that remains at 600°C, denoted as residues are recorded. It can also be observed that all three types of clay nanocomposites (2.65 vol %) show higher degradation temperature than pure PP/PS. Figure 6 shows the TGA thermograms of neat PP/PS (80/20) and nanocomposites with different modified kaolin clays at 2.65 vol %.

**Table I.** TGA Results for PP/PS (80/20) Clay Nanocomposites

Samples	10% mass loss (°C)	50% mass loss (°C)	$T_{\text{onset}}$ (°C)	$T_{\text{max}}$	Residue at 600°C (%)
Pure blend	384.76	426.60	370.49	434.39	0.4561
Blend + 2.65 vol % N100	407.23	440.14	390.75	450.09	1.5
Blend + 2.65 vol % N100V	407.83	446.42	397.30	460.65	1.774
Blend + 2.65 vol % N100A	411.02	445.03	395.10	456.77	1.09

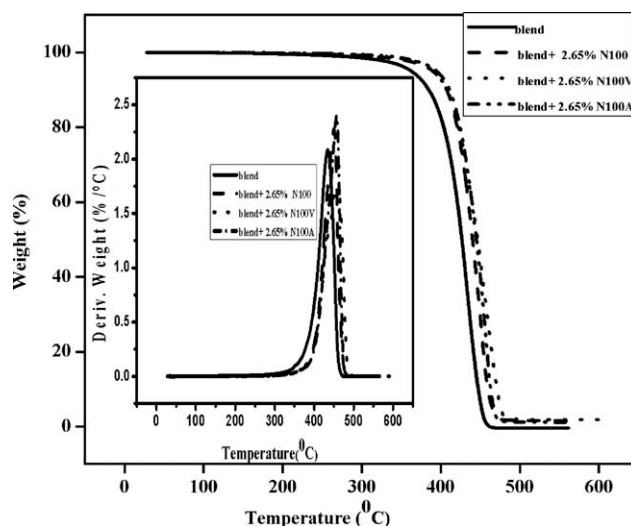


**Figure 6.** TGA thermograms of neat PP/PS (80/20), PP/PS/N100, PP/PS/N100V, and PP/PS/N100A.

The decomposition temperature of the clay nanocomposites increases in the order N100, N 100A, and N100 V. Pure blend shows an onset degradation temperature of 370°C. For the unmodified clay this temperature shifts to 390°C, the corresponding value for vinyl and amino modified clay nanocomposites are 397 and 395°C, respectively. Improved thermal stability of nanocomposites can be attributed to the decreased permeability of oxygen caused by the partial exfoliation of the clay in the nanocomposites. This may result in the formation of highly charred carbonaceous silicate cumulating on the nanocomposites surface. The charred surface layer formed during decomposition shields the thermal shock due to heat penetration to the underlying material; on the other hand such cumulative char layer tends to retard diffusion of  $O_2$  and volatile products through nanocomposites.<sup>22–24</sup> The temperature at which weight loss reaches 50% drastically shifts to higher temperatures upon the addition of clay.

### Dynamic Mechanical Behavior

DMA is used to study the relaxation in polymers. The DMA measurement consists of the observation of time-dependent deformation behavior of a sample under periodic mostly sinusoidal deformation force with very small amplitudes. Thus, it is possible to calculate storage modulus  $E'$  and loss factor  $\tan \delta$  as a function of temperature and deformation frequency. The analysis of storage modulus and  $\tan \delta$  curves is very useful in ascertaining the performance of the sample under cyclic stress and temperature. Figure 7 compares dynamic storage modulus



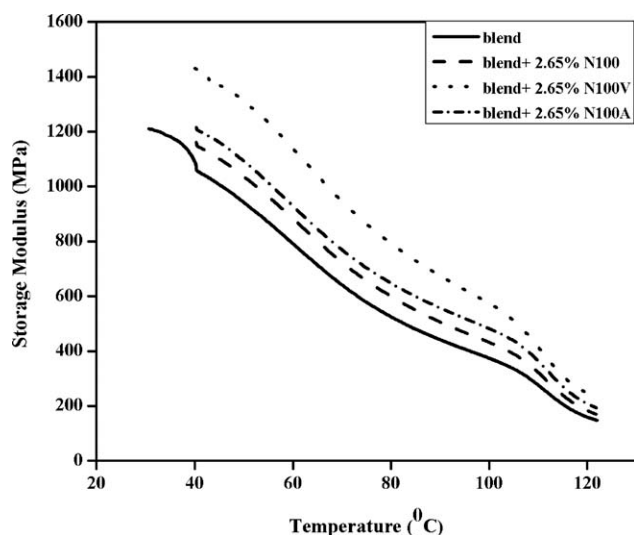


**Figure 7.** Storage modulus curves for PP/PS (80/20), PP/PS/N100, PP/PS/N100V, and PP/PS/N100A.

curves of nanocomposites with different modified kaolin clays at 2.65 vol % with PP/PS pure blend. PP/PS clay nanocomposites exhibit higher storage moduli over the entire temperature range of the study (40–125°C). As can be seen from the figure, the nanocomposites with vinyl silane modified clay (N100 V) shows noticeably higher values of storage modulus over the range of temperature. This further shows the overall superiority of the vinyl silane modified kaolin clay in improving the mechanical behavior of the blend. This observation clearly illustrates the effect of intercalation of the polymer in clay layers, leading to dispersion of clay platelets in the polymer matrix. The enhancement of storage modulus strongly depends on the aspect ratio of the dispersed clay particles and the intercalation of the polymer chains inside the clay matrix.<sup>25–27</sup> When a polymer matrix is reinforced with rigid filler particles, the polymer interface adjacent to the clay particle is highly restrained mechanically. Active surface area of the filler increases because of the intercalation of the polymer chains inside the clay galleries.

Polymer chains inside the clay galleries are immobilized and the effective immobilization of these chains is responsible for the enhancement of the hydrodynamic storage modulus. Figure 8 shows the variation of  $\tan \delta$  [ratio of loss to storage modulus ( $E''/E'$ )] is plotted as a function of temperature. The  $\tan \delta$  curves represent the ratio of dissipated energy to stored energy and relates to the  $T_g$  of the polymer.  $\tan \delta$  is useful in determining the occurrence of molecular mobility transitions such as  $T_g$ . From the figure it can be observed that there is a slight decrease in  $T_g$  with the addition of nanoclays. The reduction is attributed to the plasticizing action of the various surfactants of

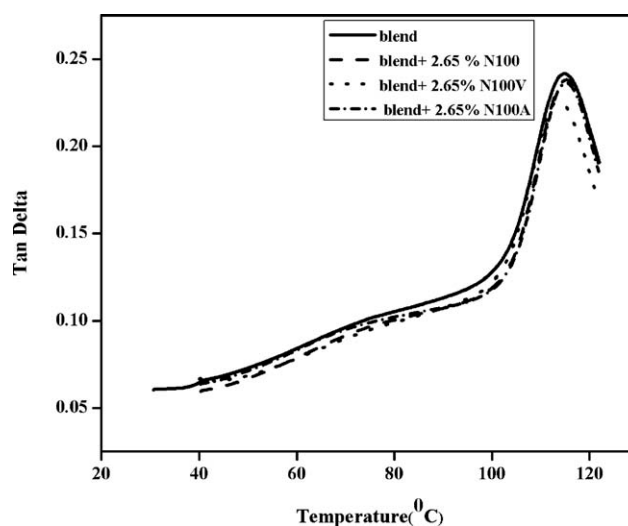


**Figure 8.**  $\tan \delta$  peaks for PP/PS (80/20), PP/PS/N100, PP/PS/N100V, PP/PS/N100A.

organically modified clays. Such plasticizing action may be responsible for the improved mobility of polymer chains, which cause reduction of  $T_g$ .<sup>28</sup> Table II shows the  $T_g$  values obtained for the pure PP/PS blend and the modified nanocomposites from the  $\tan \delta$  curves.

### Scanning Electron Microscopy

The changes in the phase morphology of PP/PS (80/20) blend with different types of clay modification at 2.65 vol % are shown in the Figure 9. On the basis of the morphology of organoclay, we can explain how the silane modification of the clay edges affects the dispersion process of clay particles in a polymer matrix. The morphology of the fractured cross sections of the tensile samples is demonstrated in Figure 9. PP/PS pure blend [Figure 9(a)] exhibits a morphology in which spherical domains of PS phase are surrounded by the continuous PP phase, and the interface between the spherical domains and the PP matrix shows weak interfacial adhesion between two phases.

The PP/PS/N100 nanocomposite [Figure 9(b)] contains aggregates of micro sized particles, which shows weak interfacial interaction. SEM observation shows that the clays are dispersed in the polymer matrix in the form of large and small aggregates in PP/PS/N100A nanocomposites [Figure 9(d)]. The weak interface between the dispersed phase (PS) and the continuous phase (PP) results in reduction of properties in PP/PS/N100A (amino silane modified) nanocomposite. SEM micrograph of a typical homogeneous dispersion is observed in the N100V modified clay nanocomposite [Figure 9(c)]. On the other hand by adding N100V (vinyl silane modified clay) the adhesion between two components can be improved to form a homogeneous

**Table II.** Glass Transition Temperatures Measured by DMA

Samples	Pure blend	Blend + 2.65 vol % N100	Blend + 2.65 vol % N100V	Blend + 2.65 vol % N100A
$T_g$ (°C)	114.95	114.67	114.35	114.11

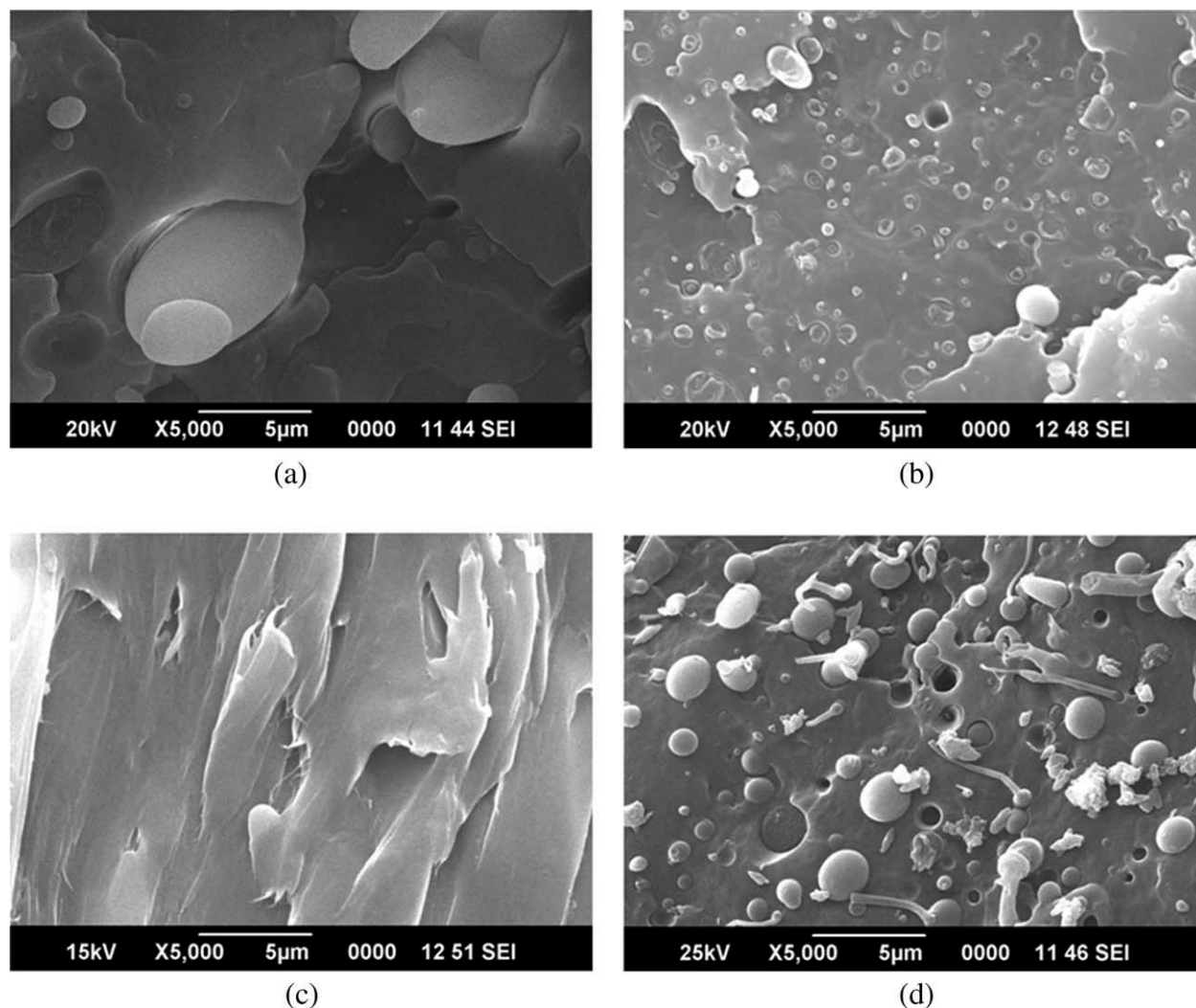


**Figure 9.** SEM images of (a) PP/PS neat blend, (b) PP/PS/N100, (c) PP/PS/N100V, and (d) PP/PS/N100A.

morphology. Therefore, the improved homogeneity increases the tensile and flexural properties. This is in complete agreement with the observed mechanical properties and the XRD results in which the nanocomposites with this modified clay exhibit the highest interlayer spacing. The nanocomposites prepared using vinyl silane modification exhibits better dispersion of clay layers within the polymer matrix than the unmodified as well as amino silane modified clay.

## CONCLUSIONS

The vinyl silane modified nanocomposite is found to have an intercalated structure having much superior thermal stability and dynamic mechanical properties. The dynamic mechanical analysis reveals higher storage moduli for the modified clay nanocomposites over the entire temperature range, and the extent of increase in the storage modulus is dependent on the type of clay modification. The nanocomposites with vinyl silane modified clay (Nanocaliber 100 V) show noticeably higher values of storage modulus over the range of temperature studied. In Nanocaliber100V modified nanocomposite system, the clay layers are delaminated as thin

platelets in the matrix as evidenced by the shifting of diffraction peaks to lower angle in XRD region. PP/PS/N100 shows 11% increase in tensile strength while PP/PS/N100V and PP/PS/N100A show 23% and 17% increase, respectively than pure PP/PS blend. SEM micrograph shows better dispersion for PP/PS/N100V nanocomposite and the dispersion of the particles in polymer matrix is influenced by the strength of interaction between polymer and filler and also the type of modification. The dispersion of clay particle is also found to improve with proper modification.

## REFERENCES

- Xuening, L.; Nan, H. *Sci. Chin. Ser. B: Chem.* **2005**, *48*, 326.
- Zhang, Q.; Gao, X.-L.; Wang, K.; Fu, Q. *Chin. J. Polym. Sci.* **2004**, *22*, 175.
- Kim, K. Y.; Ju, D. U.; Nam, G. J.; Lee, J. W. *Macromol. Symp.* **2007**, *249*, 283.
- Kim, D. H.; Park, J. U.; Cho, K. S.; Ahn, K. H.; Lee, S. J. *Macromol. Mater. Eng.* **2006**, *291*, 1127.

5. Dong, Y.; Bhattacharyya, D. *Composites*. **2008**, *39*, 1177.
6. You, C.-J.; Jia, D.-M. *Chin. J. Polym. Sci.* **2003**, *21*, 443.
7. Samsudin, S. A.; Hassan, A.; Mokhtar, M.; Jamaludin, S. M. *S. Jurnal Teknologi* **2003**, *39*, 35.
8. Hung, C.-J.; Chuang, H.-Y.; Chang, F.-C. *J. Appl. Polym. Sci.* **2008**, *107*, 831.
9. Brostow, W.; Grguric, T. H.; Olea-Mejia, O.; Rek, V.; Unni, J. *e-Polymers*. **2008**, *33*, 145.
10. Zhu, Y.; Ma, H.-Y.; Tong, L.-F.; Fang, Z.-P. *J. Zhejiang Univ. Sci. A* **2008**, *11*, 1614.
11. Ray, S. S.; Pouliot, S.; Bousmina, M.; Leszek, A. *Utracki Polym.* **2004**, *45*, 8403.
12. . Zykova, J.; Kalendova, A.; matejka, V.; Zadraba, P.; Malac, J. *Advances in sensors, signals and materials-conference 2010*; University of Algarve, Faro, Portugal.
13. Elbokl, T. A.; Detellier, C. J. *Phys. Chem. Solids*. **2006**, *67*, 950.
14. Zhang, Q.; Liu, Q.; Mark, J. E.; Noda, I. *Appl. Clay Sci.* **2009**, *46*, 51.
15. Ares, A.; Pardo, S. G.; Abad, M. J.; Cano, J.; Barral, L. *Rheol. Acta*. **2010**, *49*, 607.
16. Ryu, J. G.; Kim, H.; Lee, J. W. *Polym. Eng. Sci.* **2004**, *44*, 1198.
17. Li, J.; Li, H.; Wu, C.; Ke, Y.; Wang, D.; Li, Q.; Zhang, L.; Hu, Y. *Eur. Polym. J.* **2009**, *45*, 2619.
18. Ellis, T. S.; D'Angelo, J. S. *J. Appl. Polym. Sci.* **2003**, *90*, 1639.
19. Jiang, X. L.; Sun, K.; Zhang, Y. X. *Express Polymer Lett.* **2007**, *1*, 283.
20. Zhang, X.; Loo, L. S. *J. Polym. Sci. B: Polym. Phys.* **2008**, *46*, 2605.
21. Nelson, J. K.; Zenger, W.; Keefe, R. J.; Schadler Feist, L. S. US Pat. no. 7,579,397B2.
22. Kiersnowski, A.; Trelinska-Wlazalk, M.; Dolega, J.; Piglowski, J. *e-Polymers*. **2006**, *072*.
23. Sanchez-Valdes, S.; Mendez-Nonell, J.; Ramos de valle, L. F.; Lozano-Ramierz, T.; Ramirez-Vargas, E.; Lopez-Quintanilla, M. L.; Gutierrez-Rodriguez, J. M. *e-Polymers*. **2009**, *126*.
24. Sharma, S. K.; Nayak, S. K. *Polym. Degrad. Stab.* **2009**, *94*, 132.
25. Ataefard, M.; Moradian, S. *Polym. Plast. Technol.* **2011**, *50*, 732.
26. Ray, S. S.; Okamoto, M. *Progr. Polym. Sci.* **2003**, *28*, 1539.
27. Yu, D.; Bhattacharyya, D.; Hunter, P. J. *Compos. Sci. Technol.* **2008**, *68*, 2864.
28. Zhua, Y.; Maa, H.-Y.; Tonga, L.-F.; Fang, Z.- P. *Chin. J. Polym. Sci.* **2008**, *26*, 783.